

# ***In situ* electrochemical constructing of Co/CoP crystalline-amorphous hetero-phase catalysts for highly efficient electrocatalytic hydrogen evolution**

Yali Wu,<sup>a</sup> Di Gao,<sup>a</sup> Lu Huang,<sup>a</sup> Huihui Shi,<sup>a</sup> Peixin Yang,<sup>b</sup> Jiangna Guo,<sup>a</sup>  
Ming Zhou,<sup>\*,a</sup> Peng Xiao<sup>\*,b</sup> and Yunhuai Zhang<sup>\*,a</sup>

<sup>a</sup> College of Chemistry and Chemical Engineering, Chongqing University, Chongqing  
401331, China

<sup>b</sup> Chongqing Key Laboratory of Soft Condensed Matter Physics and Smart Materials,  
College of Physics, Chongqing University, Chongqing 401331, China

† Electronic supplementary information (ESI) available.

## **Corresponding Authors:**

(Y. H. Zhang) [zyh2031@cqu.edu.cn](mailto:zyh2031@cqu.edu.cn);

(P. Xiao) [xiaopeng@cqu.edu.cn](mailto:xiaopeng@cqu.edu.cn);

(M. Zhou) [mingzhou@cqu.edu.cn](mailto:mingzhou@cqu.edu.cn);

## **1. EXPERIMENTAL SECTION**

### **1.1. Chemicals and Materials.**

Cobalt chloride hexahydrate ( $\text{CoCl}_2 \cdot 6\text{H}_2\text{O}$ , 99%), potassium chloride (KCl, 99%), sodium hypophosphite ( $\text{NaH}_2\text{PO}_2$ , 99%) were purchased from Sigma-Aldrich Corporation. All chemicals were used as received without further purification. Titanium (Ti) foils (500  $\mu\text{m}$  thick, 99%) were obtained from Wenghou Metal Materials Corporation (Hefei province, China), and was then cutted into small wafers with an area of  $1 \times 2 \text{ cm}^2$  for use during electrodeposition. All electrodeposition solutions were freshly prepared using DI water with a resistance of  $18.25 \text{ M}\Omega \cdot \text{cm}$  (purified through a Millipore system).

### **1.2. Electrochemical Deposition of Co/CoP Crystalline-Amorphous Hetero-Phase Catalysts.**

Electrodeposition solution was firstly prepared by mixed 0.05 M  $\text{NaH}_2\text{PO}_2$ , 0.05 M  $\text{CoCl}_2 \cdot 6\text{H}_2\text{O}$ , and 20 mL of deionized water in a beaker and magnetically stirred for 15 min to enable forming a clear precursor solution. Note that  $\text{NaH}_2\text{PO}_2$  was used as the phosphorus source, pH regulator and metal ions stabilizer in the electrodeposition bath. Secondly, the Co/CoP hetero-phase catalysts were electrochemically deposited onto the Ti foil in a standard three-electrode glass setup using an electrochemical workstation (CHI660D). A graphite sheet (1 cm  $\times$  1 cm), Ag/AgCl (sat. KCl), and a piece of Ti wafer were acted as auxiliary, reference, and working electrodes, respectively. Particularly, prior to the deposition, the Ti foil was pretreated ultrasonically with HCl (18 wt.%) for 15 min to completely remove the surface oxide layer, followed by

subsequent sonication in ethanol. During electrodeposition, Ti foil electrode was immersed in the bath with an infiltrated area of 1 cm<sup>2</sup>. The as-deposited catalysts were obtained by applying cyclic voltammetry technique in a voltage range of -1.2 to -0.2 V vs. Ag/AgCl at a scan rate of 5 mV s<sup>-1</sup> for 3 cycles, 5 cycles, 10 cycles, 15 cycles, and 20 cycles, respectively. After electrodeposition, the as-obtained catalysts were immediately removed from the deposition solution and placed in water to rinse off the residues absorbed on the surfaces for 1.5 h. Lastly, the supported catalysts were dried under a stream of N<sub>2</sub> and then in vacuum at 60 °C for 10 h. Specifically, the mass loadings on the Ti substrate were determined using a microbalance based on the difference in mass before and after the electrodeposition.

### **1.3. Materials Characterizations.**

The size, morphology and microstructure of the samples were characterized by field emission scanning electron microscopy (FE-SEM, Nova 400 Nano-SEM) and high-resolution transmission electron microscope (HRTEM, Thermo Fischer Talos F200<sub>x</sub>, 200 kV). X-ray diffraction (XRD) patterns were recorded on Bruker D8 advanced X-ray diffractometer operating at 40 kV equipped with a Cu K $\alpha$  radiation ( $\lambda = 1.5418 \text{ \AA}$ ). X-ray photoelectron spectroscopy (XPS) spectra were obtained on a photoelectron spectroscopy (XPS, ESCALAB250, Thermo Fisher Scientific) with Mg K $\alpha$  excitation source was employed to analyze the valence states of each element. The resultant spectra were analysed by pre-calibrating the peak positions in terms of the standard C 1s peak (284.6 eV), and then subtracting the noise background and well-fitting each peak using an Avantage software.

#### 1.4. Electrochemical Measurements.

All the electrochemical measurements of as-obtained catalysts were performed on a computer-controlled CHI660D electrochemical workstation and conducted in a typical three-electrode configuration. The as-deposited catalysts on Ti foil, graphite plate, and an Ag/AgCl (sat. KCl) were served as working, counter, and reference electrodes, respectively. All the reported potentials herein were converted into reversible hydrogen electrode (RHE) based on the following equation:

$$E \text{ (vs. RHE)} = E \text{ (vs. Ag/AgCl)} + E_{\text{Ag/AgCl}}^{\theta} + 0.059 \times \text{pH}$$

where  $E_{\text{Ag/AgCl}}^{\theta} = 0.197 \text{ V vs. RHE}$  at 298 K. Prior to electrochemical measurements, 1 M KOH solutions with a pH value of 13.7 were continuously purged with 99% N<sub>2</sub> for 40 min. Linear sweep voltammetry (LSV) curves were carried out at a sweep rate of 5 mV s<sup>-1</sup>. Note that all current densities were normalized to the geometrical area of the working electrode. To assess the HER kinetics, the Tafel plots can be obtained by plotting the overpotential ( $\eta$ ) against log current ( $\log j$ ) based on the polarization curves. Notably, 90% internal resistance ( $IR$ ) compensation was typically adopted in all the LSV experiments to eliminate the voltage drop between the working and reference electrodes. The electrochemically active surface areas (ECSAs) of the as-prepared catalysts were assessed using cyclic voltammetry (CV) technique at different scanning rates (10, 20, 30, 40 and 50 mV s<sup>-1</sup>). Especially, the ECSAs of the as-prepared catalysts was calculated in terms of following equation:

$$\text{ECSAs} = C_{\text{dl}}/C_s$$

where  $C_{\text{dl}}$  and  $C_s$  are the electrochemical double-layer capacitance and specific capacitance of the samples, respectively. Electrochemical impedance spectra (EIS)

were recorded in a frequency range from 0.01 to 100 kHz with a perturbation amplitude of 5 mV.

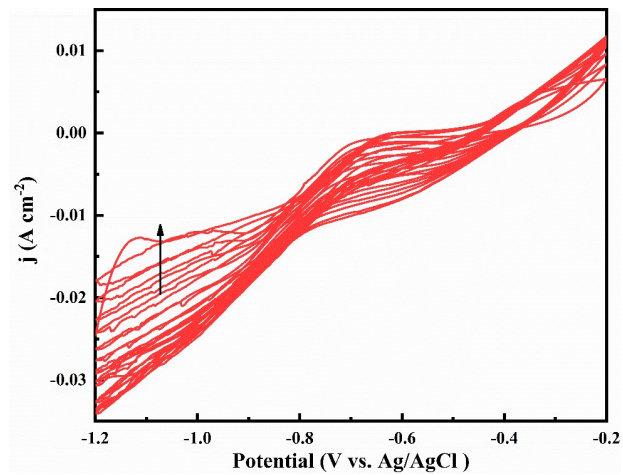


**Fig. S1.** Electrodeposition curves recorded using cyclic voltammograms at a scan rate of  $5 \text{ mV s}^{-1}$  in the electrolyte containing  $\text{Co}^{2+}$  and  $\text{H}_2\text{PO}_2^-$ .

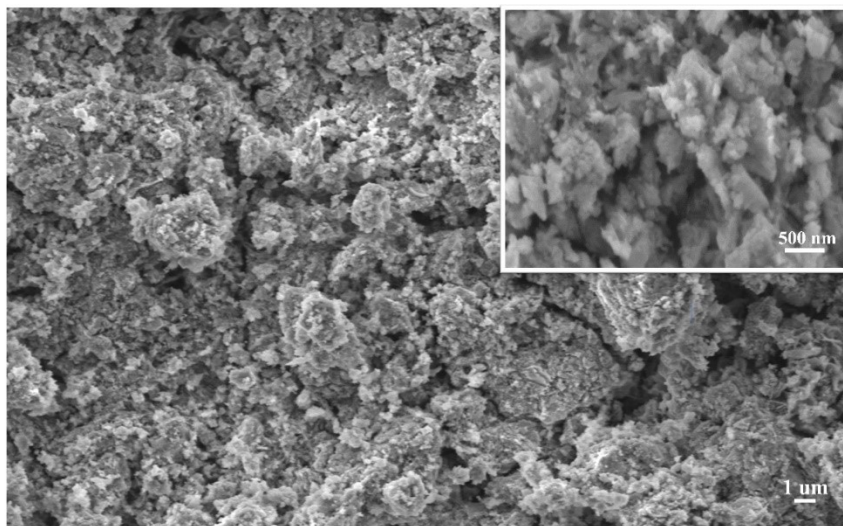


**Fig. S2.** SEM image of as-synthesized catalysts by electrodepositing in a voltage range from -1.2 to -0.2 V vs. Ag/AgCl at a scan rate of 5 mV s<sup>-1</sup> for 3 cycles. The inset shows the high-magnification SEM image.

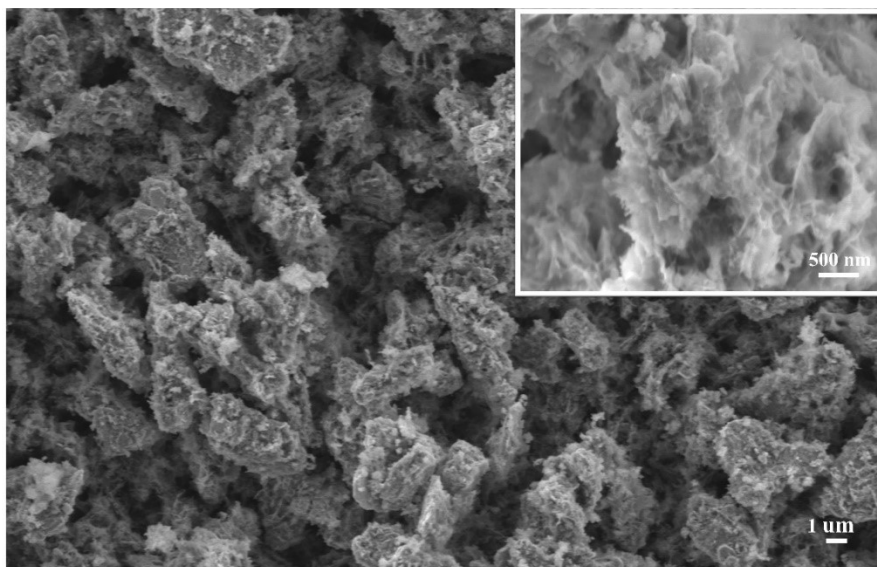


**Fig. S3.** SEM image of as-synthesized catalysts by electrodepositing in a voltage range from -1.2 to -0.2 V vs. Ag/AgCl at a scan rate of  $5 \text{ mV s}^{-1}$  for 5 cycles. The inset shows the high-magnification SEM image.



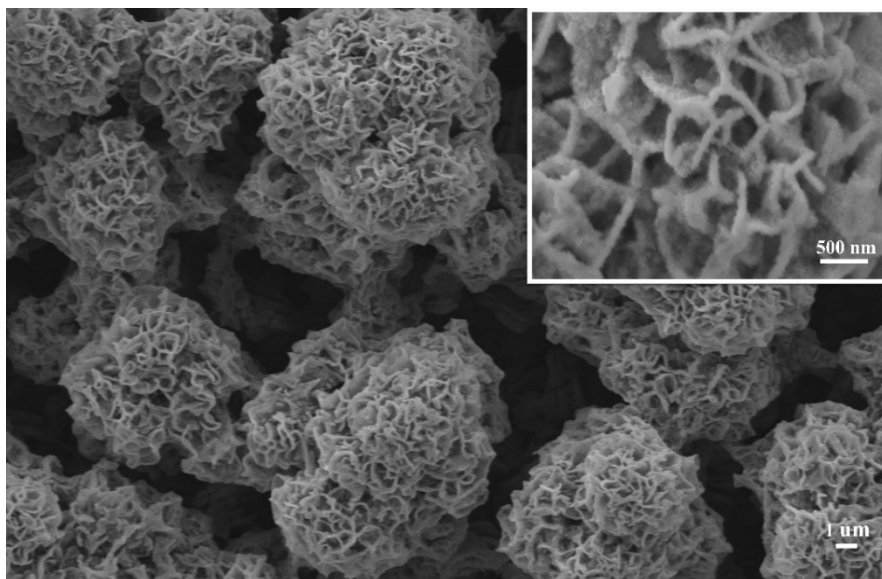


**Fig. S4.** SEM image of as-synthesized catalysts by electrodepositing in a voltage range from -1.2 to -0.2 V *vs.* Ag/AgCl at a scan rate of 5 mV s<sup>-1</sup> for 10 cycles. The inset shows the high-magnification SEM image.

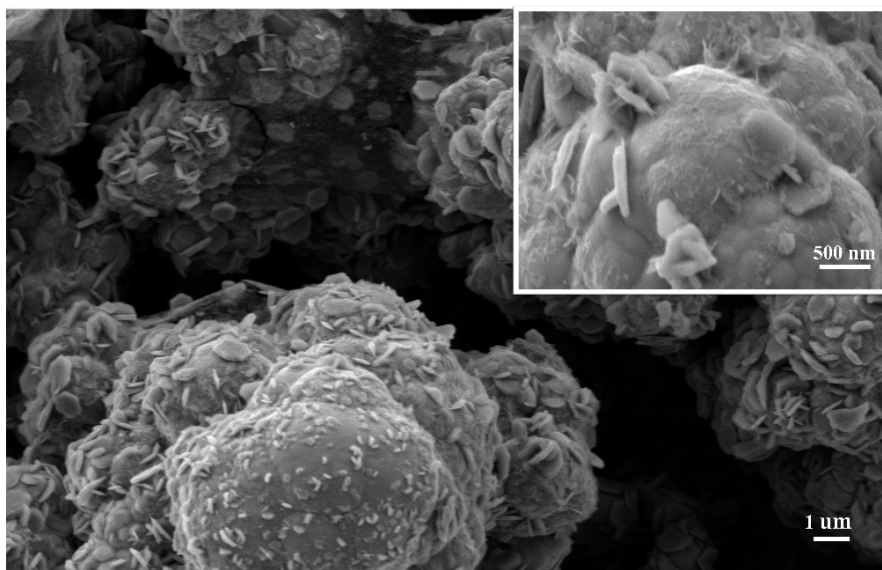


**Fig. S5.** SEM image of as-synthesized catalysts by electrodepositing in a voltage range from -1.2 to -0.2 V *vs.* Ag/AgCl at a scan rate of 5 mV s<sup>-1</sup> for 20 cycles. The inset shows the high-magnification SEM image.

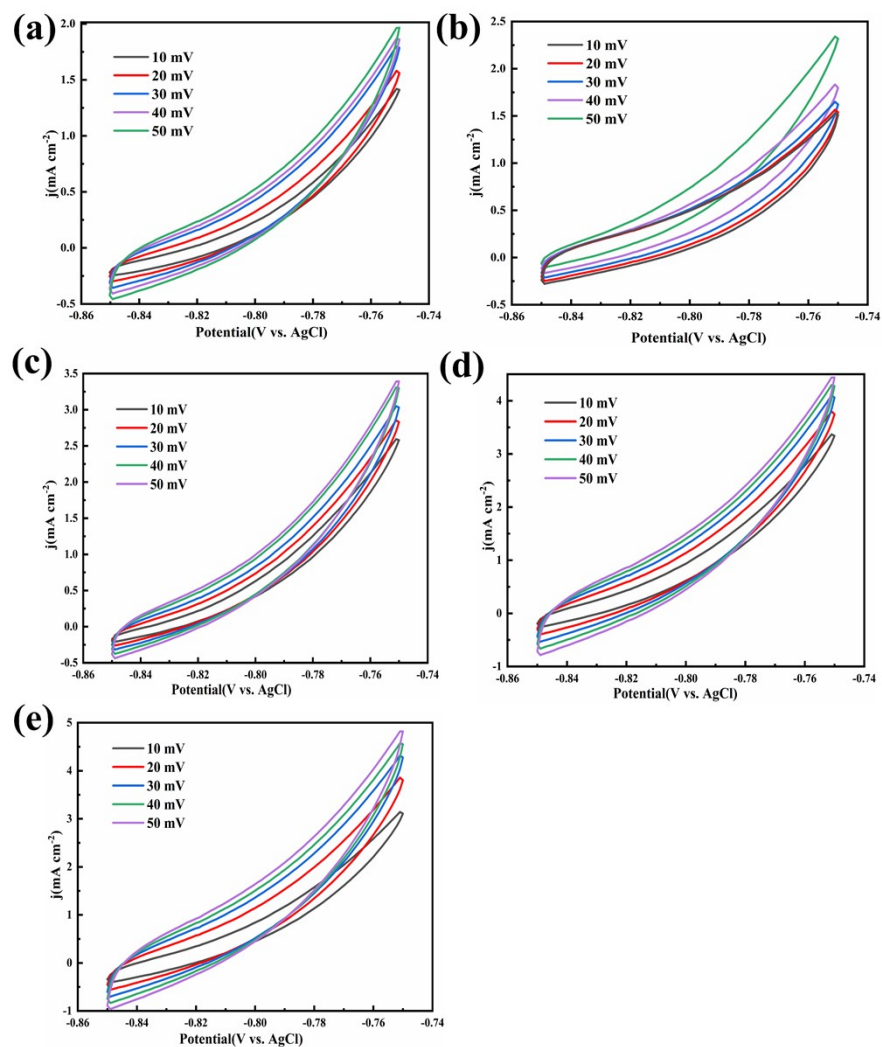


**Fig. S6.** CVs of the as-deposited catalysts prepared by scanning (a) 3 cycles, (b) 5 cycles, (c) 10 cycles, (d) 15 cycles and (e) 20 cycles in a non-Faradaic region with various scan rates from 10 to 50  $\text{mV s}^{-1}$  in 1 M KOH solution.

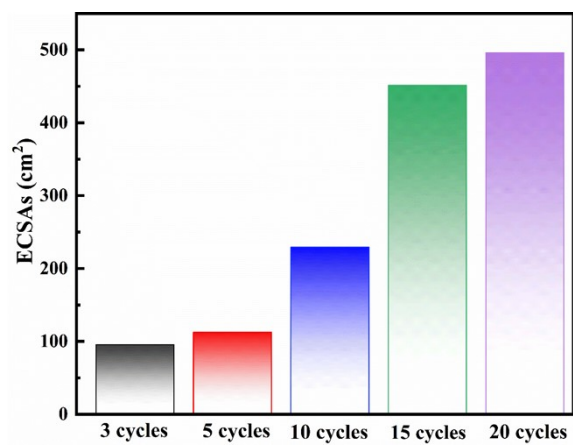


**Fig. S7.** The electrochemical active surface areas (ECSAs) of the as-deposited catalysts prepared under different conditions.

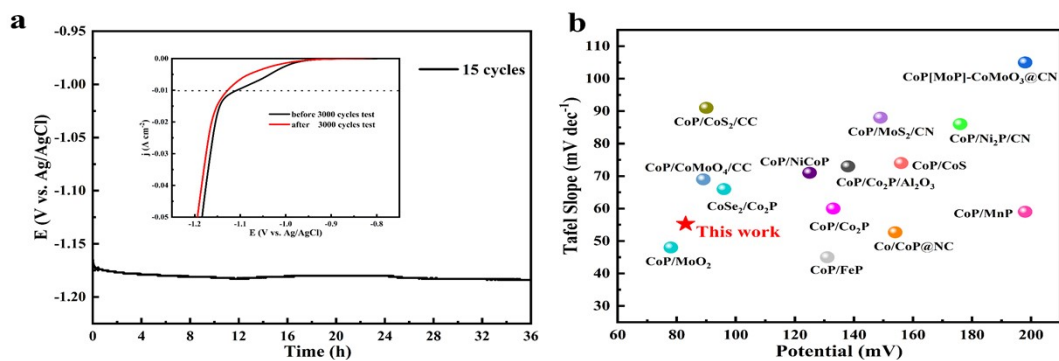


**Fig. S8.** (a) Chronopotentiometry measurement of Co/CoP catalysts depositing for 15 cycles at a static current density of  $-10 \text{ mA cm}^{-2}$  for 36 h in 1 M KOH solution. The inset shows LSV curves of the catalysts before and after 3000 cycles test. (b) Overpotential at a current density of  $10 \text{ mA cm}^{-2}$  and Tafel slope comparisons of as-deposited catalysts in our work relative to previously reported CoP based electrocatalysts.

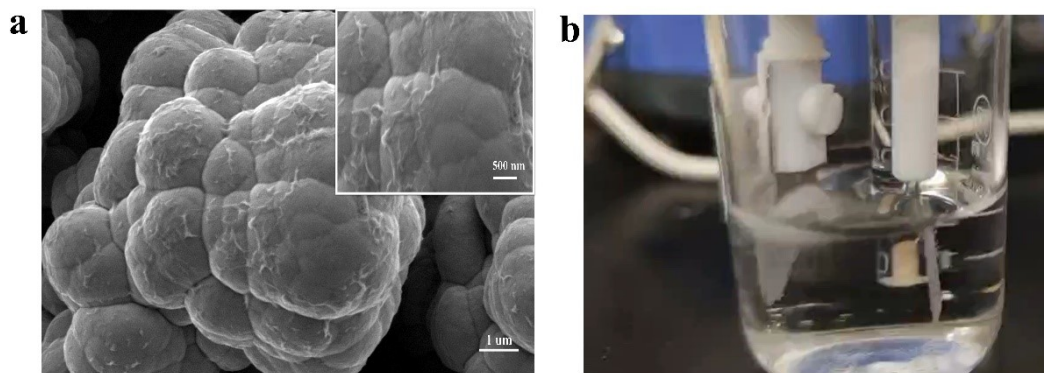


**Fig. S9.** (a) SEM image of as-deposited Co/CoP hetero-phase electrocatalysts (prepared by scanning 15 cycles) after the stability test. (b) Digital picture of HER device. The inset in (a) shows the high-magnification SEM image.

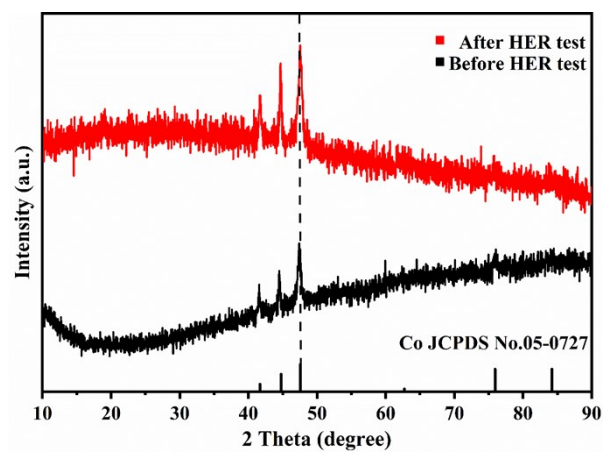


**Fig. S10.** XRD patterns of Co/CoP hetero-phase electrocatalyst (15 cycles) before and after HER measurement.

**Table S1.** Summary of the  $C_{dl}$ , ECSAs, roughness, loading mass and specific surface area.

<b>Catalysts</b>	<b><math>C_{dl}</math> (mF cm<sup>-2</sup>)</b>	<b>ECSAs (cm<sup>2</sup>)</b>	<b>Roughness</b>	<b>Loading mass (mg cm<sup>-2</sup>)</b>	<b>Specific surface area (cm<sup>2</sup> mg<sup>-1</sup>)</b>
3 cycles	3.82	95.5	95.5	1.5	63.7
5 cycles	4.51	112.75	112.75	1.7	66.3
10 cycles	9.17	229.25	229.25	3.2	71.6
15 cycles	18.06	451.5	451.5	3.7	122.0
20 cycles	19.84	496	496	3.9	127.2



**Table S2.** The exchange current density  $j^0$  of the catalysts

---

$$\eta = a + b \log j; \quad a = (2.3RT/\alpha F) \log j^0; \quad b = 2.3RT/\alpha F$$

---

Catalysts	a	b	$j^0$ (mA cm <sup>-2</sup> )
3 cycles	0.13043	0.08449	0.029
5 cycles	0.09921	0.05905	0.029
10 cycles	0.06608	0.06492	0.096
15 cycles	0.04466	0.0653	0.207
20 cycles	0.06578	0.04995	0.048

---

**Table S3.** Potential at a current density of 10 mA cm<sup>-2</sup> and Tafel slope comparisons of the previously reported electrocatalysts containing earth-abundant elements.

<b>Catalysts</b>	<b>Potential (mV) @10mA cm<sup>-2</sup></b>	<b>Tafel Slope (mV dec<sup>-1</sup>)</b>	<b>Reference</b>
CoP/Co	83	55.3	This work
CoP/Co <sub>2</sub> P	133	60	J. Power Sources, 2021, 486, 229351.
CoP/CN@MoS <sub>2</sub>	149	88	ACS Appl. Mater. Interfaces, 2019, 11, 36649–36657.
CoP/MoO <sub>2</sub>	78	48	Int. J. Hydrogen Energy, 2021, 46, 18353-18363.
CoP/Ni <sub>2</sub> P/CN	176	86	Int. J. Hydrogen Energy, 2021, 46, 8431-8443.
CoP/NiCoP	125	71	Adv. Energy Mater., 2019, 9, 1901213.
CoP/CoS	156	74	ChemCatChem, 2019, 11, 6099-6104.
CoP/FeP	131	45	Int. J. Hydrogen Energy, 2019, 44, 19978-19985.
CoP/MnP	198	59	Int. J. Hydrogen Energy, 2019, 44, 19978-19985.
CoSe <sub>2</sub> /Co <sub>2</sub> P	96	66	Dalton Trans., 2021, 50, 6650-6658.
CoP/CoS <sub>2</sub> /CC	90	91	Electrocatalysis, 2019, 10, 253-261.
CoP/CoMoO <sub>4</sub> /CC	89	69	J. Mater. Sci. Technol., 2020, 46, 177-184.
CoP/CoP <sub>2</sub> /Al <sub>2</sub> O <sub>3</sub>	138	73	Nanoscale, 2017, 9, 5677.
CoP (MoP)- CoMoO <sub>3</sub> @CN	198	105	ACS Appl. Mater. Interfaces, 2019, 11, 6890- 6899.
Co/CoP@NC	154	52.7	Energy Storage Mater., 2018, 12, 44-53.